

Perylene as an Organic Photocatalyst for the Radical Polymerization of Functionalized Vinyl Monomers through Oxidative Quenching with Alkyl Bromides and Visible Light

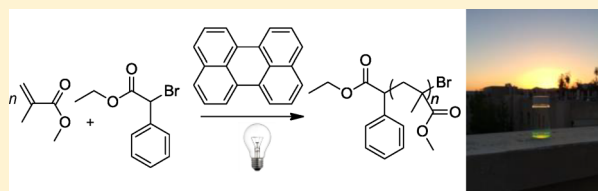
Garret M. Miyake^{*,†,‡} and Jordan C. Theriot[†]

[†]Department of Chemistry and Biochemistry, University of Colorado, Boulder, Colorado 80309-0215, United States

[‡]Arnold and Mabel Beckman Laboratories for Chemical Synthesis, Division of Chemistry and Chemical Engineering, California Institute of Technology, Pasadena, California 91125, United States

Supporting Information

ABSTRACT: The generation of carbon-centered radicals from alkyl bromides through an oxidative quenching pathway using perylene as an organic visible-light photocatalyst is described. This methodology is used to initiate the radical polymerization of methyl methacrylate and other functionalized vinyl monomers. The polymers possess bromide chain-end groups that can be used to reinitiate polymerization to produce block copolymers. Control over the polymerization propagation can be achieved through pulsed light sequences while the ability to use natural sunlight to promote carbon–carbon bond formation produces polymers with dispersity as low as 1.29.



■ INTRODUCTION

Photoinitiated homolytic decomposition of peroxide or azo compounds using intense ultraviolet light is a classic method for initiating free radical polymerization.¹ In addition to enabling low-temperature reactions, photopolymerization provides the capability for spatial and temporal control.² Although photocatalysts have been known for some time, visible-light photoredox catalysis has gained recent momentum, being recognized as a green approach for providing the opportunity to exploit sunlight to enable reactivity.³ As such, there has been increasing interest in merging the attractiveness of visible-light photopolymerization with the utility of living polymerizations.⁴

Atom transfer radical polymerization (ATRP) has emerged as the most utilized controlled radical polymerization (CRP), in part due to operational simplicity and synthetic versatility.⁵ The photoreduction of copper(II) complexes to active copper(I) catalysts implements photopolymerization into ATRP and demonstrates one approach to minimizing transition metal catalyst concentration.⁶ It has also been shown that polypyridal ruthenium⁷ and iridium⁸ photocatalysts can catalyze ATRP. In the presence of sacrificial electron donors, ruthenium complexes can activate alkyl halides through a reductive quenching pathway, whereas iridium complexes are able to directly activate alkyl halides through an oxidative quenching pathway (Figure 1). This distinction is significant because it is known that the use of sacrificial electron donors can introduce undesirable decomposition pathways,⁹ complicating the synthesis of well-defined polymers. Although metal catalyzed photo-ATRP can produce well-defined polymers and yield excellent temporal control, the polymer is inevitably contaminated with trace metal residue that raises concern for

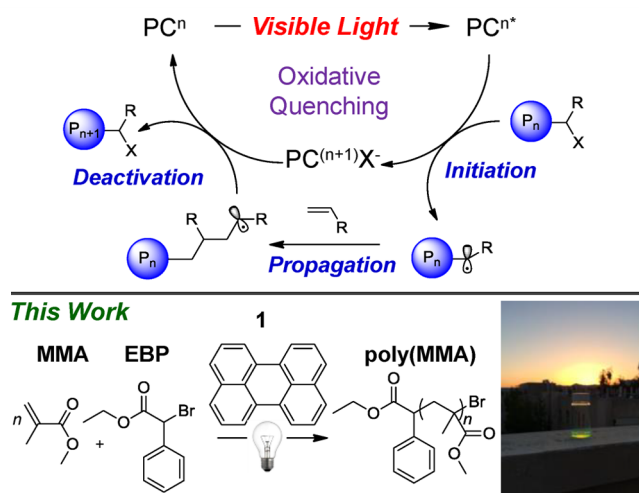


Figure 1. Proposed mechanism for a photoredox-mediated ATRP proceeding through an oxidative quenching pathway with alkyl halides (top) and the use of perylene as an organic photocatalyst for the polymerization of methyl methacrylate with alkyl bromide initiators (bottom) and a photograph of this polymerization being mediated by natural sunlight (bottom right).

biomedical or electronic applications. Therefore, there is a tremendous interest in utilizing organic photocatalysts¹⁰ in polymer synthesis.¹¹

Received: October 3, 2014

Revised: October 29, 2014

Published: November 18, 2014

Table 1. Results of the Polymerization of Methyl Methacrylate Using Perylene as the Photocatalyst^a

run no.	[MMA]:[EBP]:[1]	mol % (% 1)	solvent	time (h)	yield (%) ^b	M_w (kDa) ^c	M_n (kDa) ^c	\bar{D} (M_w/M_n) ^c	theoretical M_n (kDa) ^d	I^* (EBP) (%) ^e	I^* (1) (%) ^f
1	875:9:1	0.11	DMF	24	53.0	82.5	55.4	1.49	5.16 (46.4)	9.3	84
2	875:9:1	0.11	neat	24	68.1	328	180	1.82	6.63 (59.7)	3.7	33
3	875:9:1 ^g	0.11	DMF	10	59.2	53.1	41.2	1.29	5.76 (51.9)	14	126
4	875:9:1	0.11	CH ₃ NO ₂	24	17.8	146	95.4	1.53	1.73 (15.6)	1.8	16
5	875:9:1	0.11	DME	24	71.7	51.0	31.7	1.61	6.98 (62.8)	22	198
6	875:9:1	0.11	dioxane	24	>99	66.4	38.8	1.71	9.72 (87.5)	25	226
7	875:9:1	0.11	benzene	24	95.1	42.3	22.9	1.85	9.26 (83.3)	40	364
8	875:18:1	0.11	DMF	24	52.8	60.2	35.8	1.68	2.57 (46.3)	7.2	129
9	875:1:1	0.11	DMF	24	55.9	92.1	55.8	1.65	48.9 (48.9)	88	88
10	437:1:1	0.22	DMF	22	70.9	81.3	52.5	1.56	31.0 (31.0)	59	59
11	437:0.5:1	0.22	DMF	24	60.2	215	135	1.59	105 (52.7)	78	39
12	8750:90:1	0.011	DMF	24	63.7	173	125	1.39	6.20 (558)	4.9	446
13	87500:900:1	0.0011	DMF	24	53.4	369	253	1.46	5.20 (4678)	2.1	1849
14	875000:9000:1	0.00011	DMF	24	28.3	429	273	1.57	2.75 (24792)	1.0	9081

^aPolymerizations performed using 1.0 mL of methyl methacrylate and 1.0 mL of the solvent specified in the polymerization table (except for run no. 2, where the polymerization was run neat) and irradiated by a white LED. ^bIsolated yield. ^cMeasured using light scattering. ^dThe theoretical M_n calculated as described in ref 24 using the equivalents of monomer based on [MMA]:[EBP] or [MMA]:[1], in parentheses. ^eInitiator efficiency (I^*) calculated as described in ref 24 using the theoretical M_n based on [MMA]:[EBP]. ^fSame as footnote e, except based on [MMA]:[1]. ^gIrradiated by natural sunlight.

Visible light organic photocatalysts can also operate through reductive and oxidative quenching pathways during polymerization, with the former being more common.¹² In combination with sacrificial electron donors, excited state organic photocatalysts can mediate radical polymerizations through the reductive quenching pathway as do ruthenium complexes, with similar decomposition pathways. On the other hand, in the presence of oxidants such as iodonium salts, radicals can be generated through oxidative quenching pathways. To the best of our knowledge, no direct reduction of an alkyl bromide by an organic photocatalyst to successfully initiate polymerization has been reported.¹³ Although a truxene–acridine organic photocatalyst has recently shown to generate a carbon-centered radical through the reduction of 2-bromoacetophenone, polymerization was only observed in the presence of a sacrificial amine.¹⁴

Upon examination of the current status of organic photocatalyzed polymerization and the major limitation of traditional metal catalyzed ATRP, an apparent question arises: *can an organic photocatalyst directly reduce an alkyl bromide to generate a radical for initiating polymerization without the need for sacrificial electron donors?* Additionally, if this catalyst can reversibly deactivate a propagating radical, then an organocatalyzed variant of ATRP would be presented. Although nitroxide-mediated¹⁵ and reversible-fragmentation transfer¹⁶ radical polymerizations do not require metal catalysts, they have been less utilized than ATRP.¹⁷ Organocatalyzed variants of ATRP, for example, reversible-complexation¹⁸ and reversible chain transfer¹⁹ catalyzed polymerizations (requiring alkyl iodide initiators), are desirable.

RESULTS AND DISCUSSION

To address these questions, potential organic photocatalysts were examined in the polymerization of methyl methacrylate (MMA) using methyl α -bromoisobutyrate (MBI) as the alkyl bromide initiator.²⁰ Excitingly, perylene (1) showed promise to mediate radical polymerization through an oxidative quenching pathway. 1 is the simplest rylene dye, one of the oldest classifications of pigments. Rylene dyes are well-established,

stable colorants that have gained increasing attention in organic photovoltaics,²¹ are known to be strong reductants in their photoexcited state,²² and have found use as photoinitiators for polymerization.²³

Irradiation of a DMF solution of MMA, MBI, and 1 ([MMA]:[MBI]:[1] = 875:9:1) with a white LED for 24 h afforded poly(MMA) in 43.8% yield with a weight-average molecular weight (M_w) of 78.1 kDa and relatively low dispersity (\bar{D}) of 1.27 (run S1, Table S1). The experimentally measured molecular weight (MW) is much greater than the theoretical MW (considering [MMA]:[MBI]), giving a low initiator efficiency (I^*) of 6.9%.²⁴ This motivated the exploration of other alkyl bromides as initiators for enhancing I^* .²⁰ Replacing MBI with ethyl α -bromophenylacetate (EBP) increased the polymer yield to 47.9%, while reducing the polymer MW (M_w = 50.1 kDa), albeit with a slightly higher \bar{D} of 1.43. This increased I^* to 13% and EBP was thereafter the initiator used in this study. Reducing the DMF volume resulted in a slightly higher yield (53.0%), while producing a polymer with M_w = 82.5 kDa and \bar{D} of 1.49 (I^* = 9.3%) (run 1, Table 1).

Control experiments revealed that omission of any single component (1, EBP, or light source) resulted in no polymeric product, even after 72 h. Changing the light source to an orange LED also resulted in no polymerization, eliminating the possibility of a thermally initiated polymerization. The polymerization does not proceed in the presence of oxygen but can be run neat, producing a high-MW polymer (M_w = 328 kDa; \bar{D} = 1.82; run 2, Table 1). Natural sunlight can also be used as the light source to produce a polymer with a relatively low \bar{D} of 1.29 (run 3, Table 1).

Investigating the effects of solvent on polymerization provided the observation that, in general, less polar solvents increased the polymer yield, I^* (i.e., polymers possessed lower MWs), and \bar{D} (runs 4–7, Table 1). For example, when nitromethane was used as the solvent, the resulting polymer was isolated in a low 17.8% yield, with a high M_w of 146 kDa (I^* = 1.8%, run 4, Table 1). When the polymerization was performed in benzene, the polymer product was isolated in 95.1% yield (M_w = 42.3 kDa; I^* = 40%, run 7, Table 1). Unfortunately, this was accompanied by a large increase in \bar{D} to

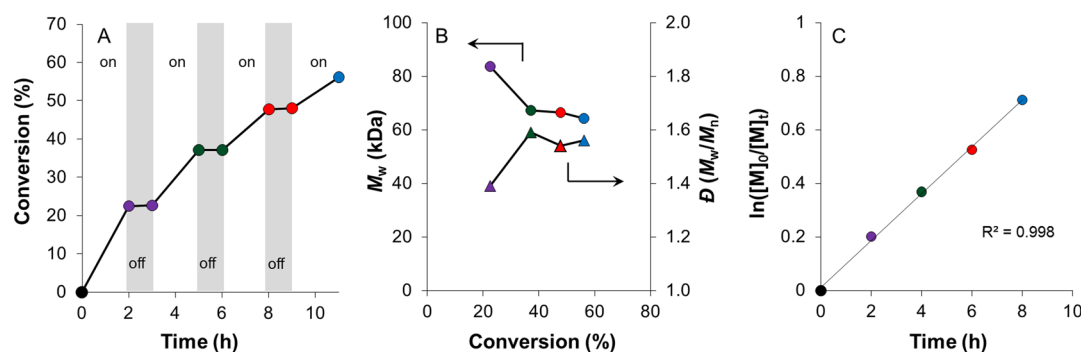


Figure 2. (A) Plot of monomer conversion vs time demonstrating the control over polymerization propagation through irradiation (white regions) and removal of the light source (shaded regions). (B) Plot of the molecular weight and molecular weight dispersity as a function of monomer conversion after the first (purple), second (green), third (red), and fourth (blue) irradiation periods. (C) First-order kinetic plot of monomer conversion vs time for the “on/off” light irradiation experiment. Performed in 1.00 mL of DMF and 1.00 mL (0.935 mmol) of MMA. [MMA]:[EBP]:[1] = 875:9:1.

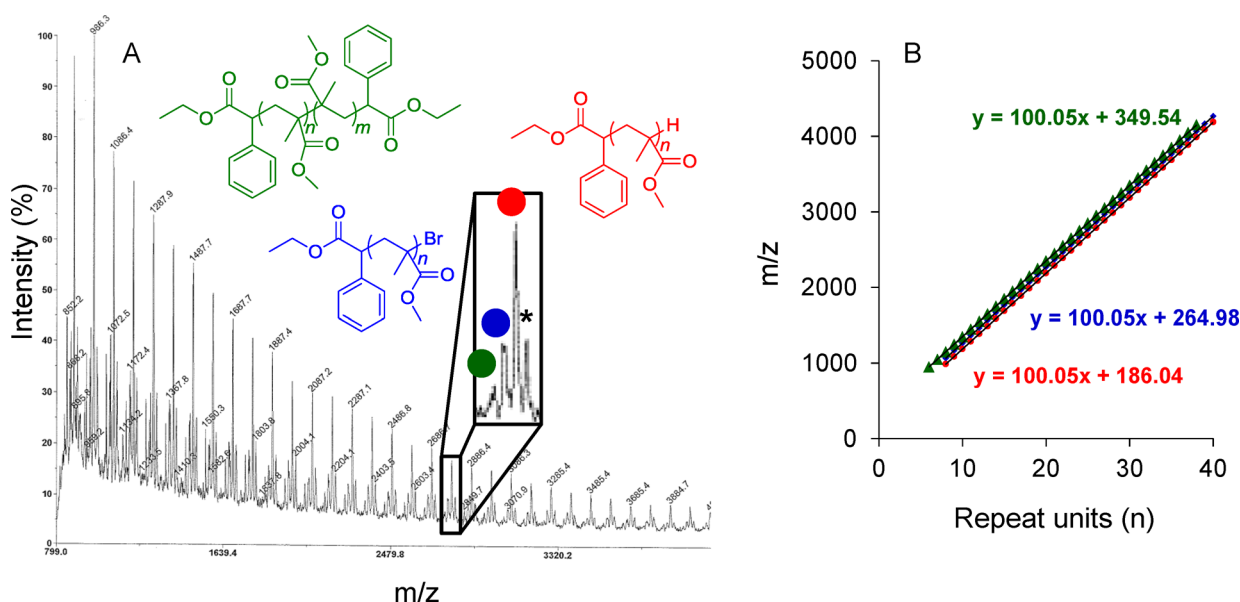


Figure 3. (A) MALDI-TOF spectra of a poly(MMA) oligomer and structural assignment of the oligomer, including the chain-end groups. Asterisk indicates unassigned peak. (B) Plot of mass-to-charge ratio (m/z) vs number of monomer repeat units from the results of MALDI-TOF analysis of a poly(MMA) oligomer. The slope of the best-fit trend line corresponds to the molecular weight of methyl methacrylate repeat unit while the y -intercept indicates the molecular weight of the poly(MMA) chain-end groups.

1.85. Thus, further efforts to improve the efficiency of polymerization and gain insight into this polymerization were made utilizing DMF as the solvent.

To confirm the necessity of light for polymerization propagation, a pulsed light sequence was introduced to demonstrate temporal control. A repeated cycle of 2 h of irradiation followed by an hour of a “dark” period was performed using a ratio of [MMA]:[EBP]:[1] = 875:9:1. An aliquot of the reaction was analyzed for monomer conversion and MW prior to changing the light environment at each interval. This experiment confirmed that polymerization propagation is strictly controlled by light and only occurs during irradiation while no monomer consumption or change in polymer MW was observed during “dark” periods (Figure 2). Interestingly, although the monomer conversion follows first-order kinetics during irradiation, the MW of the polymer does not increase after the initial irradiation period but actually decreases.²⁰ This suggests that under these conditions monomer incorporation does not occur with chains formed

from previous irradiation sequences during reirradiation. Thus, as [MMA] continually decreases during this experiment, the MW of the polymer produced from each additional irradiation period is decreasingly lower and increases the \bar{D} of the polymer product.

To further understand this polymerization, the effects of initiator concentration on the polymerization were also investigated. Doubling the equivalents of EBP ([MMA]:[EBP]:[1] = 875:18:1) led to a slightly decreased polymer MW (M_w = 60.2 kDa; \bar{D} = 1.68, I^* = 7.2%), while decreasing the equivalents of EBP ([EBP] = [1] = 1) led to a slightly higher polymer MW (M_w = 92.1 kDa, \bar{D} = 1.65) with a much increased I^* of 88% (runs 8 and 9, Table 1). Increasing the equivalents of both EBP and 1 ([MMA]:[EBP]:[1] = 437:1:1) resulted in an increase in polymer yield to 70.9% with I^* = 59% (run 10, Table 1). Adding a substoichiometric amount of EBP ([MMA]:[EBP]:[1] = 875:0.5:1) did not increase the initiator efficiency (I^* = 78%) in comparison to when stoichiometric equivalents of EBP and 1 were used, but allowed the synthesis

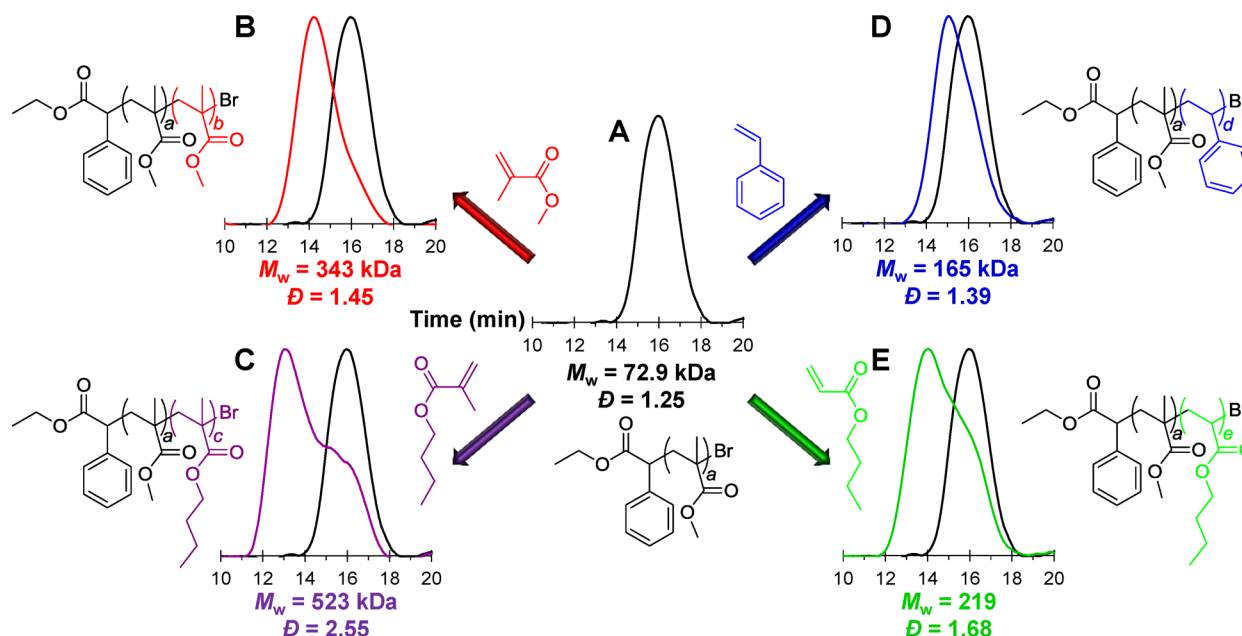


Figure 4. Chain-extension polymerizations from a poly(MMA) macroinitiator (A) with methyl methacrylate (B), butyl methacrylate (C), styrene (D), and butyl acrylate (E). Overlaid GPC traces of the poly(MMA) macroinitiator (black) with poly(MMA)-*b*-poly(MMA) (red), poly(MMA)-*b*-poly(BMA) (purple), poly(MMA)-*b*-poly(S) (blue), or poly(MMA)-*b*-poly(BA) (green).

of high-MW poly(MMA) ($M_w = 215$ kDa; $\bar{D} = 1.59$; run 11, Table 1).

These data reveal that **1** is not efficient at activating multiple equivalents of alkyl bromide initiator and brings into question the exact role of **1**. Two possibilities include (a) **1** is serving as an initiator, producing at most one polymer chain per equivalent, regardless of the equivalents of EBP employed, or (b) **1** is a catalyst that can activate multiple equivalents of initiator under appropriate conditions. To answer this question, the I^* was recalculated, disregarding the equivalents of initiator and based solely on $[MMA]:[1]$.²⁴ Through this analysis it is observed that in nonpolar solvents I^* exceeded 100%, indicating that multiple polymer chains could be initiated by **1** (runs 5–7, Table 1). To explore the possibility of increasing I^* in DMF, the catalyst loading of **1** was decreased from 110 to 0.11 mmol % (runs 12–14, Table 1). Keeping $[MMA]$ and $[EBP]$ constant and decreasing the concentration of **1** revealed that I^* could be dramatically increased under these conditions. Polymerization was still observed at low catalyst loadings of 0.11 mmol % **1**, highlighting the activity of this photo-organocatalyst, and producing a high-MW polymer ($M_w = 429$ kDa; $\bar{D} = 1.57$) with a calculated >9000 polymer chains being initiated per equivalent of **1** (run 14, Table 1). However, when considering the initiator efficiency as related to $[EBP]$, this system is inefficient ($I^* = 1.0\%$).

To understand the initiation mechanism in this polymerization, a poly(MMA) oligomer was analyzed by MALDI-TOF (matrix-assisted laser desorption ionization–time of flight). The MALDI-TOF data consisted of four sets of peaks that, among like peaks, were separated by a mass-to-charge (m/z) ratio of 100 g/mol, the molecular weight of MMA (Figure 3).

Three of the peaks could be assigned to identify the polymer chain-end groups. A minor set of peaks corresponded to poly(MMA) with both chain-end groups being ethyl 2-phenylacetate (Figure 3, green). This product is formed through radical coupling of two propagating radical chains, a potential termination reaction in radical polymerization.

Another minor set of peaks could be assigned to poly(MMA) containing an ethyl 2-phenyl acetate chain-end group while the other chain-end possessed Br, suggesting reversible deactivation is occurring to some extent with this system (Figure 3, blue). The major set of peaks is separated from the later set of peaks by a m/z ratio of 79. This set of peaks can be assigned to poly(MMA) containing an ethyl phenylacetate chain-end, but missing the Br (Figure 3, red). These data support the conclusion that polymerization initiation includes EBP but leaves to question if reversible deactivation of the propagating radical occurs to a large extent. It has been observed that during MALDI-TOF analysis Br chain-end groups can be obliterated from polymers produced by traditional ATRP.²⁵

To elucidate the extent to which Br chain-end groups are present on isolated polymers, a chain-extension experiment was performed using an isolated poly(MMA) sample ($M_w = 72.9$; $\bar{D} = 1.25$). To ensure that unreacted initiator from the polymer synthesis was removed and could not introduce the potential for an alternative initiation mechanism, the isolated polymer was redissolved into dichloromethane and reprecipitated into methanol three additional times. During each reprecipitation, the polymer was stirred in methanol for 1 h prior to filtration and extensive washing with excess methanol. This macroinitiator was dissolved in DMF and reintroduced to polymerization conditions (adding **1**, additional MMA, butyl methacrylate (BMA), butyl acrylate (BA), or styrene (S), and light).

In all cases further polymerization was observed, although a low-MW tail was observed in the GPC traces (Figure 4). For the chain extension with butyl (meth)acrylates, a large fraction of macroinitiator remained unreacted, most likely due to the lower rate of initiation with the poly(MMA) initiator, compared to polymerization propagation of the butyl (meth)acrylate monomer. However, with MMA the majority of the macroinitiator was chain-extended. In fact, the theoretical MW of the chain-extended polymer was nearly 90% of the experimentally measured MW.²⁶ The chain extension with styrene also resulted in a high percentage of macroinitiator

Table 2. Results of the Polymerization of *n*-Butyl Acrylate Using Perylene as the Photocatalyst^a

run no.	[BA]:[I]:[1]	solvent	initiator (I)	conv (%) ^b	<i>M_w</i> (kDa) ^c	<i>M_n</i> (kDa) ^c	<i>Đ</i> (<i>M_w</i> / <i>M_n</i>) ^c	theoretical <i>M_n</i> (kDa) ^d	<i>I</i> [*] (EBP) (%) ^e	<i>I</i> [*] (1) (%) ^f
15	1000:10:1	neat	EBP	71.3	28.0	20.1	1.39	9.14 (91.4)	45	455
16	1000:10:1	DMF	EBP	61.9	63.1	42.9	1.47	7.93 (79.3)	18	185
17	1000:10:1	CH ₃ CN	EBP	19.6	27.9	25.4	1.10	2.51 (25.1)	9.9	99
18	1000:10:1	DME	EBP	78.4	116	81.7	1.42	10.0 (100)	12	123
19	1000:10:1	benzene	EBP	67.9	55.4	44.7	1.24	8.70 (87.0)	19	195
20	1000:10:1	benzene	MBI	9.14	82.4	64.4	1.28	1.17 (11.7)	1.8	18
21	1000:10:1	benzene	EBF	27.7	71.3	53.2	1.34	3.55 (35.5)	6.7	67
22	1000:10:1	benzene	DBM	26.2	86.6	66.6	1.30	3.36 (35.6)	5.0	50
23	1000:10:1	benzene	DMM	61.8	61.4	46.9	1.31	7.92 (79.2)	17	169

^aPerformed in 1.00 mL of solvent (except run 15, where the polymerization was performed neat), with 1.00 mL (6.98 mmol, 1000 equiv) of BA, 1.76 mg (6.98 μmol, 1 equiv) of perylene, and 69.8 μmol (10 equiv) of the initiator specified in Table 2. Samples were irradiated by a white LED for 24 h before work-up. Initiators (I) used were ethyl α-bromophenylacetate (EBP), methyl α-bromoisobutyrate (MBI), ethyl bromodifluoroacetate (EBF), diethyl bromomalonate (DBM), and diethyl 2-bromo-2-methylmalonate (DMM). ^bMeasured by ¹H NMR. ^cDetermined by light scattering. ^dTheoretical *M_n* calculated by [BA]/[I] or [BA]/[1] (in parentheses) × polymer yield. ^eInitiator efficiency (*I*^{*}) = theoretical *M_n*/experimental *M_n* × 100 calculated using the theoretical *M_n* based on [MMA]/[I]. ^fInitiator efficiency (*I*^{*}) = theoretical *M_n*/experimental *M_n* × 100 calculated using the theoretical *M_n* based on [MMA]/[1].

conversion to block copolymer. To further eliminate the possibility that this second polymerization is initiated by something other than the macroinitiator, an extraction of the poly(MMA)-*block*-poly(BA) copolymer was performed. Poly(BA) can be separated from poly(MMA); however, homopoly(BA) was not observed, confirming that this polymerization yielded a block copolymer that was initiated from the macroinitiator.²⁷

To expand this polymerization system to other monomers, the polymerization of BA was investigated using EBP as the initiator (Table 2). The neat polymerization of BA was efficient, reaching 71.3% monomer conversion in 24 h, producing poly(BA) with a *M_w* = 28.0 kDa (*Đ* = 1.39), giving *I*^{*} = 46% (based on [BA]:[EBP]) (run 15, Table 2). A solvent screen (runs 16–19, Table 2) revealed that benzene is the best solvent for the polymerization of BA in regards to all polymerization characteristics, reaching high monomer conversion (67.9%), to produce poly(BA) with a relatively low dispersity (*Đ* = 1.24; *M_w* = 55.4 kDa). The polymerization of BA in benzene with other alkyl bromide initiators was also examined (runs 19–24, Table 2). EBP remained the best initiator, as using other initiators resulted in lower monomer conversion and polymers with larger *Đ*.

CONCLUSIONS

Perylene, known to be a strong reductant in the excited state, can serve as a photoorganocatalyst for the direct reduction of alkyl bromides to generate carbon-centered radicals for the polymerization of (meth)acrylates and styrene. A combination of MALDI-TOF and chain-extension polymerizations confirms that bromide is reinstalled onto the polymer chain-ends, supporting a reversible-deactivation polymerization mechanism. Although the current system leaves something to be desired in terms of control over the polymer molecular weight and dispersity, it shows promise as an organocatalyzed variant of ATRP. Future work will focus on gaining a mechanistic understanding of this polymerization in order to enable the rational design of more efficient catalysts for the synthesis well-defined polymers.

EXPERIMENTAL SECTION

Materials and Methods. All chemicals were purchased from Sigma-Aldrich. Methyl methacrylate (MMA), *n*-butyl methacrylate

(BMA), *n*-butyl acrylate (BA), and styrene (S) were purified by vacuum distillation. Ethyl α-bromophenylacetate (EBP), methyl α-bromoisobutyrate (MBI), ethyl bromodifluoroacetate (EBF), diethyl bromomalonate (DBM), and diethyl 2-bromo-2-methylmalonate (DMM) were degassed with one freeze–pump–thaw cycle. Perylene (sublimed grade, ≥99.5%), Eosin Y, fluorescein, and *N,N'*-bis(3-pentyl)perylene-3,4,9,10-bis(dicarboximide) were used as received. Solvents used for polymerization were sparged with nitrogen. Twelve inch Flex LED Strips-S050, Double-Density (4 W), were purchased from Creative Lighting Solutions. NMR spectra were recorded on a Varian Inova 300 MHz spectrometer. Chemical shifts were referenced to internal solvent resonances and are reported as parts per million relative to tetramethylsilane. MALDI-TOF data were provided by the California Institute of Technology Mass Spectrometry Facility. Polymer molecular weights were determined utilizing THF as the eluent (1.0 mL/min) by multiangle light scattering (MALS) gel permeation chromatography (GPC) using a miniDAWN TREOS light scattering detector, a Viscostar viscometer, and an OptilabRex refractive index detector, all from Wyatt Technology. Absolute molecular weights were determined assuming 100% mass recovery.

General Polymerization Procedure. Polymerizations were performed in a glovebox with a nitrogen atmosphere. A 20 mL vial was loaded with a stir bar and perylene, which was dissolved in the monomer and solvent, as specified in the polymerization tables. The initiator was added by syringe. For LED irradiation, the vial was placed on the center of a stir plate with one Double-Density LED Flex strip surrounding the vial in a circle with a 2.5 in. radius (Figure SI 1). The polymerization was allowed to proceed for the times specified in the polymerization tables, after which the vial was removed from the glovebox and the reaction mixture was poured into 100 mL of methanol. The mixture was allowed to stir for 1 h, and the polymer was isolated by filtration and dried under vacuum to a constant weight. For natural sunlight irradiation (performed at Caltech on the roof of Crellin Laboratory on October 5, 2013, from 8:00 am to 6:00 pm), the polymerization reaction was prepared as mentioned above in a glovebox, before the sealed vial was brought to the roof. The vial was placed on a single sheet of aluminum foil and was irradiated for 10 h without stirring. For the “on/off” light irradiation experiment, the general polymerization conditions were used, and for the “off” time periods, the reaction was placed in a metal container sealed with a metal lid. The polymer was isolated as stated above. For conversion data, a 0.2 mL aliquot was taken by syringe from the polymerization reaction and quenched into a septum sealed vial containing 0.6 mL of unpurified (i.e., not degassed) CDCl₃ containing 250 ppm BHT. ¹H NMR was used to quantify the monomer conversion. The volatiles were removed, and the residue was redissolved in THF for GPC analysis.

MALDI-TOF Analysis. The polymerization used the general conditions stated above. A 20 mL vial was loaded with a stir bar, 5.4 mg of perylene, 1.0 mL of DMF, and 1.0 mL of MMA. 3.8 μ L of EPB was added by syringe. The polymerization was irradiated by a white LED for 30 min before a 0.2 mL aliquot was injected into a vial containing 1.0 mL of unpurified methanol. The volatiles were removed, and the residue was used directly for analysis. Analysis was performed with a Voyager DE-PRO MALDI time-of-flight mass spectrometer (Applied Biosystems) equipped with a nitrogen laser. The sample was dissolved in 250 μ L of THF and diluted $\times 10$ with matrix solution (benzylidene malononitrile, 10 mg/mL in THF). To the sample was added NaI in EtOH as an ionizing agent. The instrument mass accuracy is $\pm 0.1\%$ and was externally calibrated with Sequazyme standard mixture.

Chain-Extension Polymerizations. The polymerization used the general conditions stated above. The macroinitiator was synthesized as follows. 27.0 mg of perylene (0.107 mmol, 1 equiv) and 10.0 mL of MMA (93.5 mmol, 899 equiv) were dissolved in 40.0 mL of DMF. 164 μ L of EBP (0.937 mmol, 9 equiv) was added, and with vigorous stirring the solution was irradiated with a white LED for 20 h. The solution was poured into 200 mL of methanol and stirred for 1 h. The polymer was filtered and washed with excess methanol. The polymer was redissolved into dichloromethane and reprecipitated into methanol. After isolation by filtration and washing with excess methanol, this procedure was repeated two additional times to afford 2.55 g of poly(MMA) (27.2%). The molecular weight properties of the macroinitiator were measured as described above ($M_w = 72.9$ kDa; $D = 1.25$). For chain-extension polymerization, 100 mg of the macroinitiator (1.71 μ mol, 0.87 equiv) and 0.5 mg of perylene (1.98 μ mol, 1 equiv) were dissolved in 2.00 mL of DMF and MMA (1.00 mL, 9.35 mmol, 4718 equiv), BMA (1.49 mL, 9.35 mmol, 4718 equiv), BA (1.33 mL, 9.35 mmol, 4718 equiv), or styrene (1.07 mL, 9.35 mmol, 4718 equiv) were added via syringe. The reactions were irradiated with a white LED for 20 h before the polymer was isolated as previously mentioned.

■ ASSOCIATED CONTENT

● Supporting Information

This work was supported by the University of Colorado Boulder and the Camille and Henry Dreyfus Foundation Postdoctoral Program in Environmental Chemistry. This material is available free of charge via the Internet at <http://pubs.acs.org>.

■ AUTHOR INFORMATION

Corresponding Author

*E-mail garret.miyake@colorado.edu (G.M.M.).

Notes

The authors declare no competing financial interest.

■ ACKNOWLEDGMENTS

The authors thank Drs. Harit U. Vora and Victoria A. Piunova for helpful discussions, Dr. Pablo E. Guzman for technical assistance, and Prof. Robert H. Grubbs for mentorship.

■ REFERENCES

- (1) (a) Fouassier, J.-F.; Lalevée, J. *Photoinitiators for Polymer Synthesis*; Wiley-VCH: Weinheim, Germany, 2012. (b) Yagci, Y.; Jockusch, S.; Turro, N. J. *Macromolecules* **2010**, *43*, 6245–6260.
- (2) (a) Chatani, S.; Kloxin, C. J.; Bowman, C. N. *Polym. Chem.* **2014**, *5*, 2187–2201. (b) Monroe, B. M.; Weed, G. C. *Chem. Rev.* **1993**, *93*, 435–448.
- (3) (a) Schultz, D. M.; Yoon, T. P. *Science* **2014**, *343*, 1239176. (b) Prier, C. K.; Rankic, D. A.; MacMillan, D. W. C. *Chem. Rev.* **2013**, *113*, 5322–5363. (c) Nicewicz, D. A.; Nguyen, T. M. *ACS Catal.* **2014**, *4*, 355–360. (d) Narayanam, J. M. R.; Stephenson, C. R. J. *Chem. Soc. Rev.* **2011**, *40*, 102–113. (e) Yoon, T. P.; Ischay, M. A.; Du, J. *Nat. Chem.* **2010**, *2*, 527–532. (f) Albini, A.; Fagnoni, M. *ChemSusChem* **2008**, *1*, 63–66. (g) Fagnoni, M.; Dondi, D.; Ravelli, D.; Albini, A. *Chem. Rev.* **2007**, *107*, 2725–2756.
- (4) (a) Xu, J.; Jung, K.; Atme, A.; Shanmugam, S.; Boyer, C. J. *Am. Chem. Soc.* **2014**, *136*, 5508–5519. (b) Weitekamp, R. A.; Atwater, H. A.; Grubbs, R. H. *J. Am. Chem. Soc.* **2013**, *135*, 16817–16820. (c) Yamago, S.; Nakamura, Y. *Polymer* **2013**, *54*, 981–994. (d) Ohtsuki, A.; Goto, A.; Kaji, H. *Macromolecules* **2013**, *46*, 96–102. (e) Yamago, S.; Nakamura, Y. *Polymer* **2013**, *54*, 981–994. (f) Yamago, S.; Ukai, Y.; Matsumoto, A.; Nakamura, Y. *J. Am. Chem. Soc.* **2009**, *131*, 2100–2101. (g) Koumura, K.; Satoh, K.; Kamigaito, M. *Macromolecules* **2008**, *41*, 7359–7367.
- (5) (a) Matyjaszewski, K.; Tsarevsky, N. V. *J. Am. Chem. Soc.* **2014**, *136*, 6513–6533. (b) Matyjaszewski, K. *Macromolecules* **2012**, *45*, 4015. (c) di Lena, F.; Matyjaszewski, K. *Prog. Polym. Sci.* **2010**, *35*, 959–1021. (d) Ouchi, M.; Terashima, T.; Sawamoto, M. *Chem. Rev.* **2009**, *109*, 4963–5050. (e) Matyjaszewski, K.; Tsarevsky, N. V. *Nat. Chem.* **2009**, *1*, 276–288. (f) Ouchi, M.; Terashima, T.; Sawamoto, M. *Acc. Chem. Res.* **2008**, *41*, 1120–1132. (g) Braunecker, W. A.; Matyjaszewski, K. *Prog. Polym. Sci.* **2007**, *32*, 93–146. (h) Matyjaszewski, K.; Xia, J. *Chem. Rev.* **2001**, *101*, 2921–2990.
- (6) (a) Ribelli, T. G.; Konkolewicz, D.; Bernhard, S.; Matyjaszewski, K. *J. Am. Chem. Soc.* **2014**, *136*, 13303–13312. (b) Anastasaki, A.; Nikolaou, V.; Zhang, Z.; Burns, J.; Samanta, S. R.; Waldron, C.; Haddleton, A. J.; McHale, R.; Fox, D.; Percec, V.; Wilson, P.; Haddleton, D. M. *J. Am. Chem. Soc.* **2014**, *136*, 1141–1149. (c) Konkolewicz, D.; Schröder, K.; Buback, J.; Bernhard, S.; Matyjaszewski, K. *ACS Macro Lett.* **2012**, *1*, 1219–1223. (d) Mosnáček, J.; Ilčíková, M. *Macromolecules* **2012**, *45*, 5859–5865. (e) Tasdelen, M. A.; Uygun, M.; Yagci, Y. *Macromol. Rapid Commun.* **2011**, *32*, 58–62.
- (7) Zhang, G.; Song, I. Y.; Ahn, K. H.; Park, T.; Choi, W. *Macromolecules* **2011**, *44*, 7594–7599.
- (8) (a) Treat, N. J.; Fors, B. P.; Kramer, J. W.; Christianson, M.; Chiu, C.-Y.; de Alaniz, J. R.; Hawker, C. J. *ACS Macro Lett.* **2014**, *3*, 580–584. (b) Fors, B. P.; Hawker, C. J. *Angew. Chem., Int. Ed.* **2012**, *51*, 8850–8853.
- (9) (a) Wallentin, C.-J.; Nguyen, J. D.; Finkbeiner, P.; Stephenson, C. R. J. *J. Am. Chem. Soc.* **2012**, *134*, 8875–8884. (b) Nguyen, J. D.; Tucker, J. W.; Konieczynska, M. D.; Stephenson, C. R. J. *J. Am. Chem. Soc.* **2011**, *133*, 4160–4163. (c) Furst, L.; Matsuura, B. S.; Narayanam, J. M. R.; Tucker, J. W.; Stephenson, C. R. J. *Org. Lett.* **2010**, *12*, 3104–3107.
- (10) (a) Ravelli, D.; Fagnoni, M.; Albini, A. *Chem. Soc. Rev.* **2013**, *42*, 97–113. (b) Fukuzumi, S.; Ohkubo, K. *Chem. Sci.* **2013**, *4*, 561–574. (c) Ravelli, D.; Fagnoni, M. *ChemCatChem* **2012**, *4*, 169–171.
- (11) (a) Lalevée, J.; Telitel, S.; Xiao, P.; Lepeltier, M.; Dumur, F.; Morlet-Savary, F.; Gimes, D.; Fouassier, J.-P. *Belstein J. Org. Chem.* **2014**, *10*, 863–876. (b) Lalevée, J.; Tehfe, M.-A.; Morlet-Savary, F.; Graff, B.; Dumar, F.; Gimes, D.; Blanchard, N.; Fouassier, J.-P. *Chimia* **2012**, *55*, 439–441.
- (12) Fouassier, J. P.; Allonas, X.; Burget, D. *Prog. Org. Coat.* **2003**, *47*, 16–36.
- (13) Broggi, J.; Terme, T.; Vanelle, P. *Angew. Chem., Int. Ed.* **2014**, *53*, 384–413.
- (14) Tehfe, M.-A.; Dumur, F.; Contal, E.; Graff, B.; Gimes, D.; Fouassier, J.-P.; Lalevée, J. *Macromol. Chem. Phys.* **2013**, *214*, 2189–2201.
- (15) (a) Nicola, J.; Guillaneuf, Y.; Lefay, C.; Bertin, D.; Gimes, D.; Charleux, B. *Prog. Polym. Sci.* **2013**, *38*, 63–235. (b) Hawker, C. J.; Bosman, A. W.; Harth, E. *Chem. Rev.* **2001**, *101*, 3661–3688.
- (16) (a) Moad, G.; Rizzardo, E.; Thang, S. H. *Aust. J. Chem.* **2009**, *62*, 1402–1472. (b) Moad, G.; Rizzardo, E.; Thang, S. H. *Polymer* **2008**, *49*, 1078–1131. (c) Moad, G.; Rizzardo, E.; Thang, S. H. *Aust. J. Chem.* **2006**, *59*, 669–692. (d) Moad, G.; Rizzardo, E.; Thang, S. H. *Aust. J. Chem.* **2005**, *58*, 379–410.
- (17) Moad, G.; Rizzardo, E.; Thang, S. H. *Acc. Chem. Res.* **2008**, *41*, 1133–1142.
- (18) (a) Tanishima, M.; Goto, A.; Lei, L.; Ohtsuki, A.; Kaji, H.; Nomura, A.; Tsujii, Y.; Yamaguchi, Y.; Komatsu, H.; Miyamoto, M.

Polymers **2014**, *6*, 311–326. (b) Goto, A.; Ohtsuki, A.; Ohfuji, H.; Tanishima, M.; Kaji, H. *J. Am. Chem. Soc.* **2013**, *135*, 11131–11139. (c) Goto, A.; Suzuki, T.; Ohfuji, H.; Tanishima, M.; Fukuda, T.; Tsujii, Y.; Kaji, H. *Macromolecules* **2011**, *44*, 8709–8715.

(19) (a) Goto, A.; Wakada, T.; Fukuda, T.; Tsujii, Y. *Macromol. Chem. Phys.* **2010**, *211*, 594–600. (b) Goto, A.; Tsujii, T.; Fukuda, T. *Polymer* **2008**, *49*, 5177–5185.

(20) See the Supporting Information.

(21) (a) Li, C.; Wonneberger, H. *Adv. Mater.* **2012**, *24*, 613–636. (b) Weil, T.; Vosch, T.; Hofkens, J.; Peneva, K.; Müllen, K. *Angew. Chem., Int. Ed.* **2010**, *49*, 9068–9093.

(22) Würthner, F. *Chem. Commun.* **2004**, 1564–1579.

(23) (a) Xiao, P.; Dumur, F.; Frigoli, M.; Graff, B.; Morlet-Savary, F.; Wantz, G.; Bock, H.; Fouassier, J. P.; Gigmes, D.; Lalevée, J. *Polym. J.* **2014**, *53*, 215–222. (b) Xia, P.; Dumur, F.; Graff, B.; Gigmes, D.; Fouassier, J. P.; Lalevée, J. *Macromol. Rapid Commun.* **2013**, *34*, 1452–1458. (c) Tehfe, M.-A.; Dumur, F.; Graff, B.; Gigmes, D.; Fouassier, J.-P.; Lalevée, J. *Macromol. Chem. Phys.* **2013**, *214*, 1052–1060.

(24) Initiator efficiency (I^*) = theoretical number average molecular weight (M_n)/experimentally measured $M_n \times 100$. Theoretical M_n = $[\text{monomer}]/[\text{initiator}] \times \text{MW of monomer} \times \% \text{ yield}$. The contribution of polymer chain-end groups to the theoretical M_n have been neglected in this analysis because of their nonuniform nature, which results in a slightly lower calculated I^* .

(25) Barner-Kowollik, C.; Davis, T. P.; Stenzel, M. H. *Polymer* **2004**, *45*, 7791–7805.

(26) Assuming 100% of the macroinitiator was isolated in the product after chain extension, there was 28.6% MMA conversion, with the $[\text{MMA}]/[\text{macroinitiator}] = 5452$. This provides a theoretical $M_n = 5452 \times 100.12 \text{ g/mol} \times 0.286 + 58.3 \times 10^3 \text{ g/mol} = 214 \times 10^3 \text{ g/mol}$. Therefore, $I^* = 214 \times 10^3 / 237 \times 10^3 \times 100 = 90.3\%$.

(27) Poly(BA) is soluble in hot hexanes while poly(MMA) is not. Depending on the weight incorporation of the two components, a poly(MMA)-*block*-poly(BA) copolymer may be soluble in hexanes. However, after Soxhlet extraction for 36 h with boiling hexanes no poly(BA) or copolymer was extracted, confirming that all polymers had a large composition of MMA.